Electroceramic Materials of Tailored Phase and Morphology by Hydrothermal Technology

Anderson Dias* and Virginia S. T. Ciminelli

Departamento de Engenharia Metalúrgica e de Materiais, UFMG, Rua Espírito Santo 35, Sala 206, Belo Horizonte-MG, 30160-030, Brazil

Received October 16, 2002. Revised Manuscript Received January 16, 2003

Hydrothermal technology was used to control the phase behavior and morphology of advanced electroceramics for applications as sensors, piezoelectrics, and low-loss dielectrics in microwave components. Conventional and microwave-assisted hydrothermal syntheses of perovskite-type ceramics $NaNbO_3$, $BaZrO_3$, $BaHfO_3$, $BaMg_{1/3}Nb_{2/3}O_3$, and also $PbWO_4$, were carried out in temperatures varying from 80 to 260 °C, under saturated vapor pressure. Computer simulations were employed to minimize the trial-and-error mode of synthesis. The obtained powders were structurally and morphologically characterized by X-ray diffraction, scanning and transmission electron microscopies, thermal analysis, Fourier transform infrared spectroscopy, and nitrogen adsorption technique. The results showed that selecting the appropriate feed chemistry and processing conditions could tailor both phase behavior and morphology of the ceramic particles.

Introduction

The science and technology for the production of nanostructured materials has generated great excitement and expectations in the past few years.[1] These materials contain a large fraction of interfacial component, leading to outstanding characteristics that bulk materials do not possess. Today, the answer to the fundamental question of how atomic-scale properties develop into bulk properties is crucial in nanoscience, which operates at the interface between the molecular and the bulk level. In fact, an immense academic interest, together with recent technological advances in the fabrication, characterization, and manipulation of nanostructures, will impact in the coming years the chemical, energy, electronic, and space industries.[2] Nowadays, the technology for preparation of nanopowders with superior characteristics is the basis on which conventional industries such as painting, coating, detergent, and cosmetics have obtained innovations, and on which rising industries such as information recording media, advanced ceramics, and electronics are promoted. This large interest in nanostructured powders to different user industries has meant clustering of activities according to technological themes.[1−4]

Among the existing technologies currently employed for the production of nanostructured powders, the hydrothermal technology presents many benefits, including a high degree of chemical homogeneity achieved on the molecular scale, use of mild temperatures and pressures, production of nanocrystalline powders in a single step, and elimination of high-temperature calcination and milling procedures to react and remove aggregates.[5] Today, hydrothermal technology represents the most promising route for low-cost production of advanced ceramic materials with characteristics suitable for the final application, either in batch reactors or in continuous reactors.[6] A wide range of crystalline, single, and multicomponent oxide materials can be produced by hydrothermal technology,[7] and it is also possible to synthesize transition metal compounds with unusual oxidation states, low-temperature phases, and metastable compounds.[8] A recent innovation in this technology was the introduction of microwaves into the reaction vessels to produce ceramic materials more rapidly.[9] Microwaving offers many advantages over conventional autoclave heating, including rapid heating to crystallization temperature, homogeneous nucleation, and fast supersaturation by the rapid dissolution of precipitated hydroxides, which leads to lower crystallization temperatures and shorter crystallization times.[10]

Our group works with hydrothermal processing of electroceramics for applications as magnetics, piezoelectrics, and relaxors.[11,12] These materials include dielectric (linear and nonlinear) and conductive (superconductors, conductors, and semiconductors) ceramics currently employed as capacitors, memories, sensors,

* To whom correspondence should be addressed via e-mail: anderson@demet.ufmg.br.

(1) Jose-Yacaman, M. *Metall. Mater. Trans. A* **1998**, *29*, 713.
(2) Issues in Nanotechnology, *Science* **2000**, *290*, 1453.
(3) Freemantle, M. *Chem. Eng. News* **1997**, *75*, 9.
(4) Allemann, E.; Leroux, J. C.; Gurny, R. *Adv. Drug Delivery Rev.* **1998**, *34*, 171.
(5) Yoshimura, M. *Eur. J. Solid State Inorg.* **1995**, *32*, R1.
(6) Cabenas, A.; Darr, J. A.; Lester, E.; Poliakoff, M. *J. Mater. Chem.* **2001**, *11*, 561.
(7) Byrappa, K.; Yoshimura, M. *Handbook of Hydrothermal Technology*; William Andrew Publishing: New York, 2001.
(8) Pang, G.; Feng, S.; Gao, Z.; Xu, Y.; Zhao, C.; Xu, R. *J. Solid State Chem.* **1997**, *128*, 313.
(9) Komarneni, S.; Roy, R.; Li, Q. H. *Mater. Res. Bull.* **1992**, *27*, 1393.
(10) Komarneni, S. *Proceedings of the 2nd International Conference on Solvothermal Reactions*; Takamatsu, Japan, 1996; pp 97−99.
(11) Dias, A.; Buono, V. T. L. *J. Mater. Res.* **1997**, *12*, 3278.
(12) Dias, A.; Buono, V. T. L.; Ciminelli, V. S. T.; Moreira, R. L. *J. Korean Phys. Soc.* **1998**, *32*, S1159.

10.1021/cm0210187 CCC: $25.00
Published on Web 02/20/2003

and actuators in microelectronics and communication components, devices for production control, environment monitoring, and biomedical applications, and, more recently, as solid oxide fuel cell cathodes.[13] It is well-known that the study of electroceramics is application driven and technology centered, with foundations in materials science, chemistry, and solid-state physics. The tools of the electroceramist include the majority of the elements of the periodic table, inorganics and organo-metallics, solid-state chemistry, crystallography and other structural and chemical characterization techniques, experimental physics, modeling, and device engineering. In this paper, we show that phase behavior and morphology of powders can be tailored for selected electroceramics systems by choosing the appropriate feed chemistry and processing conditions in hydrothermal syntheses. In addition to their inherent and well-known characteristics, the possibility to rationalize the design of a given hydrothermal experiment by using computer modeling is an advantage toward the better understanding of the optimized conditions for the control and production of advanced ceramic materials, minimizing the trial-and-error experiments under ideal conditions of temperature, pressure, pH, and reagent concentrations.

Lead-free perovskites ($NaNbO_3$, $BaZrO_3$, $BaHfO_3$, $BaMg_{1/3}Nb_{2/3}O_3$) and lead tungstates ($PbWO_4$) were obtained at different experimental conditions in conventional and microwave-assisted hydrothermal reactors. These ceramic systems were chosen to illustrate the versatility of the hydrothermal technology to fabricate the desired product with full control of both phase behavior and morphological characteristics of the obtained materials. Sodium niobate is a dielectric material which can be used mixed with $LiNbO_3$ to produce solid solutions with adequate properties for use in piezoelectric, pyroelectric, electrooptic, and ferroelastic applications.[14] Barium zirconate is an interesting material for the refractory industry, as well as a good substrate for the manufacturing of high-temperature superconductors, because of its structural compatibility and chemical inertia toward melts.[15] $BaHfO_3$ is a perovskite-type compound with an ideal cubic structure and electronic applications. For this compound, there is little or incomplete information.[16] $Ba(Mg_{1/3}Nb_{2/3})O_3$ is an important candidate material for application as dielectric resonators in microwave and millimeter-wave technologies because of its high permittivities and low dielectric losses.[17] Metal tungstates are another important class of electroceramics which have attracted much attention because of their important photoluminescence properties, electrical conductivity, and magnetic characteristics.[18−20] Lead tungstate has been developed for dense and fast radiators in γ-ray detectors, which could be used in high-radiation environments in future large-scale electromagnetic calorimeters at high-energy accelerators.[21,22] In this work, the fundamental issues relating to the hydrothermal processing conditions on the control of the phase behavior as well as of the morphological properties of all of these electroceramics are discussed in detail.

Experimental Section

Speciation information on the aqueous systems under study was obtained from thermodynamic multicomponent modeling by using computer software from OLI Systems, Inc.[23] The electrolyte solution model was employed to simulate the chemical reactions in a hydrothermal system submitted to a wide range of temperatures, pressures, reagent input concentrations, and chemical environments. The model simulated the existing experimental solubility data of high ionic strength systems based on their activity and osmotic coefficients. The effects of short-range forces and long-range electrostatics on the solution chemistry are also accounted.[24] The software (Corrosion and Environmental Simulation Programs) provides a refined user interface, which includes an advanced thermodynamic framework as a basis for predicting complex aqueous-based chemistry in equilibrium with vapor and solid phases at temperatures in the range 0−300 °C, pressures up to 1500 bar, and molal ionic strength in the range 0−30 *m*. Also, an extensive thermodynamic and physical property databank verified and validated from source literature is employed.[23,25]

Conventional hydrothermal syntheses were performed in 2-L floor stand reactors (Parr model 4532) equipped with turbine-type impellers and digital temperature controllers (model 4842) under temperatures ranging from 80 to 260 °C, for times of 1 and/or 4 h. Soluble salts of the elements present in the ceramic system under study were added to the vessel as aqueous solutions prior to its sealing. These solutions were prepared by using distilled and deionized water (18.2 MΩ.cm) and stoichiometric amounts of analytical grade reagents (Carlo Erba Reagenti and Fluka Chemie AG). The heating rate up to the processing temperature was maintained at 4 °C/min and a typical reactor loading of 50% of the total volume (2 L) was used. Microwave-assisted hydrothermal experiments were performed using a Milestone MLS-1200 MEGA microwave digestion system (2.45 GHz). This system operates at a maximum power of 1000 W, and power can be varied from 0 to 100% controlled by both pressure (autogenous pressure) and temperature. The syntheses occurred in double-walled digestion vessels (100 mL capacity) with an inner line and cover made of Teflon Tetrafluormethaxil (TFM) and an outer high-strength vessel shell made of Polyether ether heton (PEEK). The system was programmed to work at 1000 W, for 10 min, up to the processing temperature (200 °C) and maintained at 400 W, for 2 h, for the production of the desired ceramic powders (200±1 °C and 14.7±0.5 bar). After the hydrothermal syntheses, the products were rinsed with deionized water several times and dried at 80 °C.

Characterization. Chemical analyses were carried out in all produced powders by using atomic absorption spectrometry (Perkin-Elmer 5000) and X-ray fluorescence (Philips PW2400 sequential spectrometer, fitted with a rhodium target end window and Philips Super *Q* analytical software). To determine the nature of the crystalline phases, powder X-ray diffraction analyses were accomplished in a Philips PW1830 diffractometer with Cu Kα radiation (40 kV, 30 mA) and a graphite monochromator, from 10 to 100° 2θ at a speed of 0.02°

(13) Skinner, S. J. *Int. J. Inorg. Mater.* **2001**, *3*, 113.
(14) Von der Mühll, R.; Sadel, A.; Ravez, J.; Hagenmuller, P. *Solid State Comm.* **1979**, *31*, 151.
(15) Erb, A.; Walker, F.; Flükiger, R. *Physica C* **1995**, *245*, 245.
(16) Presa, P.; García, A. L. *J. Korean Phys. Soc.* **1998**, *32*, S682.
(17) Chen, X. M.; Suzuki, Y.; Sato, N. J. *J. Mater. Sci.: Mater. Electron.* **1994**, *5*, 244.
(18) Liao, H. W.; Wang, Y. F.; Liu, X. M.; Li, Y. D.; Qian, Y. T. *Chem. Mater.* **2000**, *12*, 2819.
(19) Alvarez-Vega, M.; Rodriguez-Carvajal, J.; Reyes-Cardenas J. G.; Fuentes, A. F.; Amador, U. *Chem. Mater.* **2001**, *13*, 3871.
(20) Sen, A.; Pramanik, P. *J. Eur. Ceram. Soc.* **2001**, *21*, 745.
(21) Nikl, M.; Bohácek, P.; Mihókova, E.; Solovieva, N.; Martini, M.; Vedda, A.; Fabeni, P.; Pazzi, G. P.; Kobayashi, M.; Ishii, M.; Usuki, Y.; Zimmerman, D. *J. Crystal Growth* **2001**, *229*, 312.
(22) Baccaro, S. *IEEE Trans. Nucl. Sci.* **1999**, *46*, 292.
(23) *Corrosion Simulation Program*; OLI Systems Inc.: Morris Plains, NJ, 1996.
(24) Lencka, M. M.; Nielsen, E.; Anderko, A.; Riman, R. E. *Chem. Mater.* **1997**, *9*, 1116.
(25) Anderko, A.; Sanders, S. J.; Young, R. D. *Corrosion* **1997**, *53*, 43.

Table 1. Crystalline Phases as a Function of Hydrothermal Temperature for the Systems Na−Nb−H_2O and Ba−Zr−H_2O, with Their Crystal System, Lattice Parameters, Space Groups, and ICDD Card Numbers

temp.	phase	structure	lattice parameter	space group	ICDD card
			Na−Nb−H_2O		
80 °C	$NaNbO_3$	cubic (lueshite)	a = 3.77 Å	*Pm*3*m* (221)	19-1221
110 °C	$Na_4Nb_6O_{17}$				21-1149
	Na_3NbO_4	cubic	a = 4.58 Å	F	22-1391
160 °C	Na_3NbO_4	cubic	a = 4.64 Å	F	22-1391
200 °C	$NaNb_7O_{18}$	orthorhombic	a = 14.00 Å, b = 26.38 Å, c = 3.71 Å	I (71)	34-1492
	$NaNbO_3$	monoclinic (natroniobite)			26-1380
240 °C	$NaNb_7O_{18}$	orthorhombic	a = 14.22 Å, b = 26.20 Å, c = 3.83 Å	I (71)	34-1492
	$NaNbO_3$	orthorhombic	a = 5.54 Å, b = 5.55 Å, c = 3.85 Å	Pbma (57)	33-1270
	$NaNbO_3$	rhombohedral	a = 5.22 Å, c = 15.87 Å	R	37-1076
			Ba−Zr−H_2O		
110 °C	$BaZrO_3$	cubic	a = 4.17 Å	*Pm*3*m* (221)	6-0399
	Ba_2ZrO_4	tetragonal	a = 4.18 Å, c = 13.6 Å	*I*4/*mmm* (139)	24-0130
	$Ba_3Zr_2O_7$	tetragonal	a = 4.15 Å, c = 22.9 Å	*I*4/*mmm* (139)	24-0131
140 °C	$BaZrO_3$	cubic	a = 4.175 Å	*Pm*3*m* (221)	6-0399
	Ba_2ZrO_4	tetragonal	a = 4.20 Å, c = 13.1 Å	*I*4/*mmm* (139)	24-0130
	$Ba_3Zr_2O_7$	tetragonal	a = 4.17 Å, c = 22.2 Å	*I*4/*mmm* (139)	24-0131
170 °C	$BaZrO_3$	cubic	a = 4.18 Å	*Pm*3*m* (221)	6-0399
200 °C	$BaZrO_3$	cubic	a = 4.20 Å	*Pm*3*m* (221)	6-0399

2θ/s. The morphological properties were determined by using scanning electron microscopy (JEOL 5410) at 15−25 kV with energy-dispersive spectrometry (Noran-Voyager 3050 with Norvar detector window and Si−Li X-ray detector crystal), electrical sensing zone method (Coulter Multisizer II) and gas adsorption measurements (Quantachrome NOVA1000), which have the additional ability to quantify the internal area, including pore-size distribution. Also, samples were prepared for examination by transmission electron microscopy (Philips CM200 microscope operated at 200 kV) by dispersing the powders in ethanol and dipping a carbon-coated copper grid into the dispersion. After removing the grid from the suspension, the alcohol was allowed to evaporate. Thermal analyses were conducted in Shimadzu equipment (TGA-50H and DSC-50) using alumina crucible and nitrogen as purging gas. During the analyses, the temperature was increased from room temperature to 1100 °C at a constant rate of 10 °C/min. Fourier transform infrared spectroscopy (FTIR) was also employed to characterize the ceramic materials by using a Perkin-Elmer 1760X with diffuse reflectance apparatus (micro sample cup), pyroelectric DTGS room-temperature detector, and beam splitter KBr. Mid-infrared spectra were obtained in the scan range 400−4000 cm^{-1} (60 scans per sample) with a resolution of 0.5 cm^{-1} (KBr was used a internal reference).

Results and Discussion

Structural Phase Control. In this work, the perovskite-type systems Na−Nb−H_2O and Ba−Zr−H_2O were chosen to illustrate the power of the hydrothermal technology to obtain different crystalline phases depending upon the processing conditions employed. For these systems, there are few papers and no systematic works on hydrothermal synthesis. Aqueous solutions of sodium hydroxide, niobium chloride, barium chloride hydrate, and zirconium oxychloride hydrate were used according to the system under study. Hydrothermal syntheses occurred in temperatures ranging between 80 and 240 °C, for 4 h, according to the procedures described in the preceding section. Many compounds with different crystallographic structures compose the Na−Nb−H_2O system. The goal was to control the hydrothermal conditions in order to obtain perovskite-type $NaNbO_3$, which presents the most interesting properties for use in technological applications.[14] Table 1 presents the crystallographic information about the phases observed in the present work as a function of the hydrothermal conditions for this ceramic system. It was observed that the crystallographic phases changed drastically as the hydrothermal temperature increased. Low temperatures (80 °C) favored the formation of cubic $NaNbO_3$ (lueshite-type), whereas a mixture of cubic Na_3NbO_4 and $Na_4Nb_6O_{17}$ was observed at 110 °C. The increase in the hydrothermal temperature promoted the stabilization of the phase Na_3NbO_4, leading to the total disappearance of the $Na_4Nb_6O_{17}$ at 160 °C. Two different crystallographic phases were detected at 200 °C: $NaNb_7O_{18}$ and monoclinic $NaNbO_3$ (natroniobite). Finally, at 240 °C, we have detected the presence of $NaNb_7O_{18}$ with two other $NaNbO_3$ structural phases: orthorhombic and rhombohedral.

Figure 1 presents yield diagrams obtained by computer simulations from thermodynamic data at 80 °C (Figure 1a) and 110 °C (Figure 1b) at a concentration ratio Na/Nb = 1.0. These fundamental thermodynamic studies are often employed as a predictive tool of the ceramic phase behavior in different aqueous environments.[23−25] The solid and dotted lines in the diagrams in Figure 1 represent the stability regions of solid and aqueous species, respectively. As can be seen, the perovskite phase $NaNbO_3$ could be obtained through a wide pH range and reagent concentrations at 80 °C (the

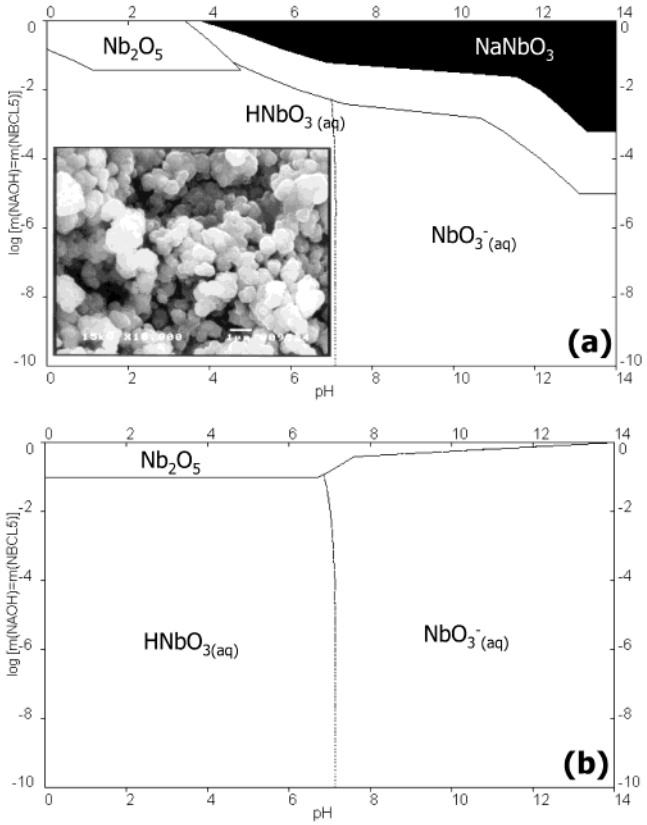

Figure 1. Yield diagrams at 99% for $NaNbO_3$ ceramics obtained by computer simulations under different pH and input reagent concentrations (Na/Nb = 1) at (a) 80 °C and (b) 110 °C. The inset in (a) is a scanning electron micrograph for a sample obtained at 80 °C for 4 h.

shaded area represents the stability region for a yield higher than 99%). In fact, computer simulations showed that cubic $NaNbO_3$ (lueshite-type) could be produced only at temperatures below 100 °C. The increase in the hydrothermal temperature leads to the stabilization of the solid-phase Nb_2O_5 (an undesirable phase) in acidic conditions as well as of the aqueous species NbO_3^- at higher reagent concentrations, which diminishes the yield of $NaNbO_3$. As it can be observed in Figure 1b for the simulations conducted at 110 °C, the solid-phase $NaNbO_3$ disappeared completely, while the stability region of the solid-phase Nb_2O_5 increased. The fact that cubic $NaNbO_3$ can be produced at temperatures below 100 °C means that an open vessel, i.e., without pressure to maintain the solution phase, can be employed. The inset in Figure 1a presents a micrograph obtained by scanning electron microscopy for a sample produced at 80 °C under optimized hydrothermal conditions (inside the shaded area). Nanostructured materials were obtained with soft agglomeration, as also observed in other ceramic materials produced by hydrothermal processing.[11,12]

Another ceramic system was chosen to show the versatility of the hydrothermal processing to control the phase behavior during synthesis. Among the ceramics of the system $Ba-Zr-H_2O$, cubic $BaZrO_3$ presents the most important properties for applications as piezoelectrics and substrate materials for high-temperature superconductors.[15] In the present work, different hydrothermal conditions were employed to study the phase behavior, and the goal was to fabricate ideal cubic

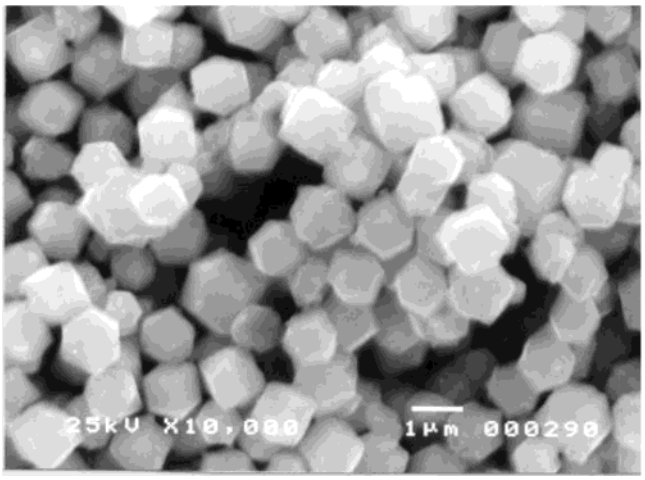

Figure 2. Scanning electron micrograph for the $BaZrO_3$ produced by hydrothermal processing at 200 °C for 4 h.

barium zirconates. As it can be seen in Table 1, the system $Ba-Zr-H_2O$ presented a clear tendency to favor the production of ideal cubic perovskites ($BaZrO_3$) for increasing hydrothermal temperatures. Also, higher temperatures promoted the stabilization of the perovskite-type phase in the $Ba-Zr-H_2O$ system. Computer modeling of the hydrothermal synthesis from thermodynamic data was carried out to understand the properties of the precursors at the temperature range studied. The results of the simulations predicted the existence of many zirconium aqueous species (Zr^{+4}, $ZrOH^{+3}$, $Zr(OH)_2^{+2}$, $Zr(OH)_3^+$) in acidic conditions, which are present in much smaller amount than the species $Zr(OH)_5^-$ (the dominant species for pH > 6). Nevertheless, in the presence of HCl (the titrant used in the present work to control the pH value), zirconia solid phase (ZrO_2) will become unstable with respect to soluble zirconium chloride complexes. By adding Cl^-, it was possible to hinder the formation of zirconia through the complexation of zirconium and chloride ions, prior to the introduction of NaOH for the precipitation of barium zirconate at high pH values. Similar results were observed by Lencka et al.[24] during the hydrothermal synthesis of $SrZrO_3$, and also by Komarneni et al.,[26] who studied the $BaZrO_3$ synthesis by both conventional and microwave-assisted hydrothermal methods. In the present work, it was verified that low reaction temperatures produced zirconates of different crystallographic structures: cubic ($BaZrO_3$) and tetragonal (Ba_2ZrO_4 and $Ba_3Zr_2O_7$) materials at 110 °C. Increasing hydrothermal temperatures promoted the stabilization of the ideal cubic phase with increasing lattice parameters (Table 1). Figure 2 presents a scanning electron micrograph for the sample produced at 200 °C for 4 h. As it can be seen, ideal cubic particles were obtained, which represent a morphological control during hydrothermal processing that will be discussed in the following paragraphs.

Morphological Control for Shaped Materials. Now that the current problems of the phase control are outlined, it becomes important to study the morphological control during hydrothermal synthesis. For the

(26) Komarneni, S.; Li, Q.; Stefansson, K. M.; Roy, R. *J. Mater. Res.* **1993**, *8*, 3176.

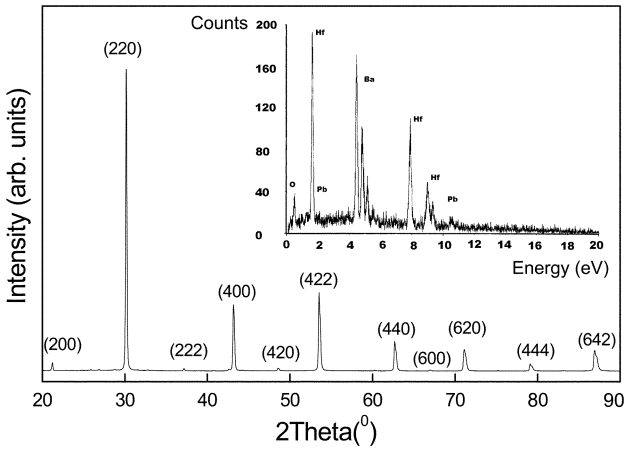

Figure 3. X-ray diffraction pattern for the hydrothermal $BaHfO_3$ ceramics. Inset: Energy-dispersive spectrometry for the sample produced at 200 °C for 4 h.

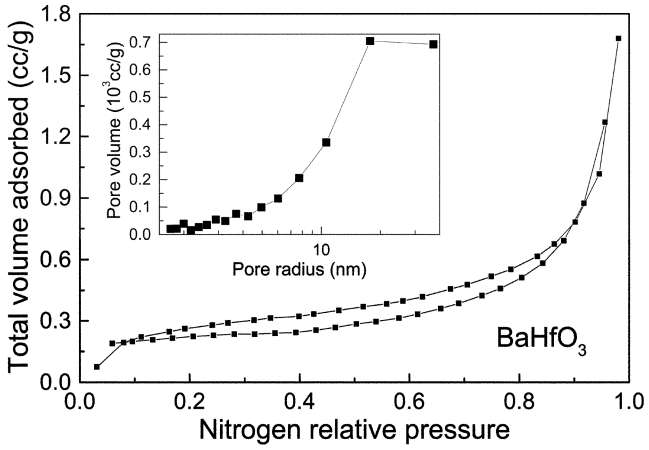

Figure 4. Nitrogen adsorption/desorption isotherms obtained at 77 K for $BaHfO_3$ powders. Inset: Pore-size distribution from the desorption curve in the capillary condensation region.

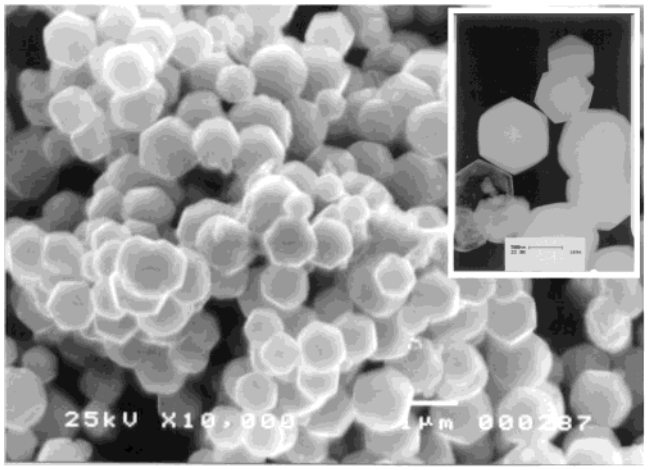

Figure 5. Scanning electron micrograph for the hydrothermal $BaHfO_3$ powders synthesized at 200 °C for 4 h. Inset: Transmission electron micrograph for the same sample.

ceramic systems discussed below, the crystalline phase obtained after synthesis is the most relevant from the point of view of the final application and, therefore, the structural phase control can be assumed as fully achieved. Now, the emphasis will be given to the hydrothermal conditions for morphological control, i.e., control over the particle size, particle shape, specific surface area, and porosity features. Again, the knowledge of the solution chemistry was a key factor to control these properties, which affect the reactivity of the particles during sintering. Initially, the results for the ceramic perovskite-type $BaHfO_3$ are presented, which constitute, to our knowledge, the first reported data on hydrothermal synthesis of these electroceramics. $BaHfO_3$ was obtained starting from hafnium oxychloride hydrate, barium chloride hydrate, and NaOH as raw materials, at 200 °C, for 4 h. Figure 3 presents the X-ray diffraction pattern (International Centre for Diffraction Data; ICDD card 24-0102), showing that crystalline and single-phase materials were obtained. The inset in Figure 3 displays the results of the energy-dispersive spectrometry analysis, showing an impurity-free powder. Thermal stability of the ceramic phase was studied by thermogravimetric analysis (TGA) and differential scanning calorimetry (DSC). As chemical reactions and many physical transitions are connected with the generation or consumption of heat, calorimetry is a universal method for investigating such processes. TGA results showed a gradual mass loss in the temperature range 200−800 °C (total mass loss equal to 3.2 wt %) attributed to physisorbed water, hydroxyl groups, and gases caught by the sample from its environment, as previously observed in other hydrothermal powders.[5,11,12] No phase transformation or decomposition was detected in the hydrothermal powders by DSC analyses and X-ray diffraction, which was carried out in thermal treated samples.

The adsorption of nitrogen onto ceramic materials is a primary method by which the morphology of powders is characterized, being a direct function of the processing conditions. Knowledge of the surface area, pore volume, and pore size distributions is further employed to design catalysts, adsorbents, and nanostrutured powders that will be sintered.[27] In this work, nitrogen adsorption analyses at 77 K were done to evaluate the morphological properties from the relationship between the volume adsorbed and the nitrogen relative pressure. Figure 4 presents the adsorption/desorption isotherms obtained for the $BaHfO_3$ ceramics. The powders presented a typical mesoporous isotherm (multilayer adsorption followed by capillary condensation) with a hysteresis characteristic of open cylindrical pores.[27] The pore-network structure was also determined from the pore-size distribution displayed as the inset in Figure 4. The mesopore distribution was calculated by using the Barrett, Joyner, and Halenda method from the desorption curve in the capillary condensation region.[27] In this method, the adsorption in mesopores is pictured as multilayer adsorption and filling of pores at a relative pressure determined by the pore diameter, whereas desorption is pictured as capillary evaporation followed by thinning of the multilayer. The results showed a large pore-size distribution with pores between 10 and 30 nm dominating the pore-network structure. The specific surface area (S_{BET}) was determined from the "knee" of the adsorption isotherm at low relative pressures as $S_{BET} = 1.0$ m^2/g. Figure 5 presents a scanning electron micrograph for the hydrothermal $BaHfO_3$ ceramics produced at pH 13. For this pH value, the synthesized particles seem to exhibit a polyhedral

(27) Dias, A.; Ciminelli, V. S. T. *Ferroelectrics* **2000**, *241*, 9.

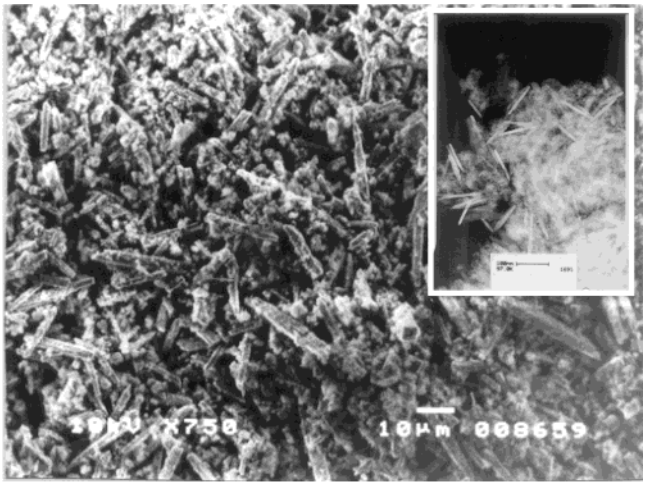

Figure 6. Scanning electron micrograph for the BMN sample obtained by microwave-assisted hydrothermal processing at 200 °C for 2 h. Inset: Transmission electron micrograph for the BMN powder produced by conventional synthesis at 200 °C for 4 h.

shape, which represents the intrinsic crystallographic habits associated with the unit cell of the material, in a minimum surface free energy configuration.[5,28] The inset in Figure 5 shows a transmission electron micrograph for this ceramic, which confirms its polyhedral shape for individual particles with sizes of about 500 nm. Materials produced at lower pH values were formed by particles of rounded-like or not-faceted shape, and more hardly agglomerated. Thus, it seems that a very high pH value is necessary to obtain shaped $BaHfO_3$ ceramics under hydrothermal conditions. It is important to emphasize that the results presented above are the first known report on the hydrothermal synthesis of barium hafnate, and therefore these may contribute to the understanding of the phase and morphological control for these electroceramics.

Now, the morphological control was extended to complex perovskite-type compounds with strong possibilities for application as dielectric resonators in microwave devices for telecommunication systems.[17] Barium magnesium niobates (BMN) were obtained by conventional and microwave-assisted hydrothermal processing at 200 °C for 4 h (conventional synthesis) and for 2 h (microwave reactors). The reagents employed were $BaCl_2 \cdot 2H_2O$, $MgCl_2 \cdot 6H_2O$, and $NH_4H_2[NbO(C_2O_4)_3] \cdot 3H_2O$, and the pH was controlled by adding NaOH until the value 13.5 was reached. The X-ray diffraction analysis showed no structural differences between the materials: both ceramic powders are crystalline and single phase (indexed by the ICDD card 17-0173) with no impurities, as verified by X-ray fluorescence and energy-dispersive spectrometry analyses. However, the morphology changed drastically depending upon the reactor used: the powders produced in conventional reactors were formed by nanometer-sized needles that could just be seen through transmission electron microscopy (inset in Figure 6), whereas the microwave-hydrothermal powders are formed by larger needle-shape materials, as shown in Figure 6. It is important to point out here the effect of the microwave heating on

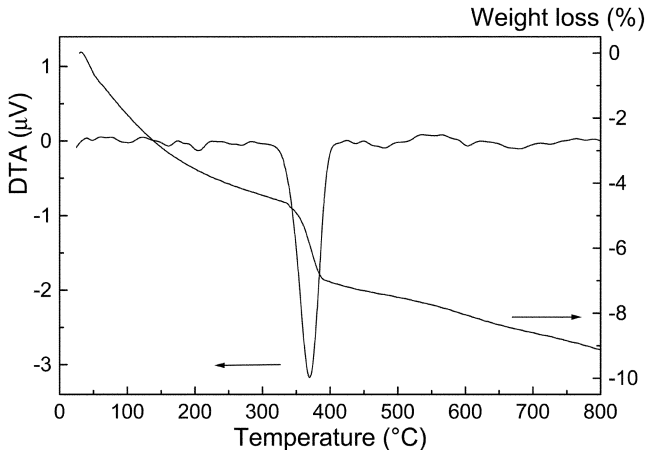

Figure 7. Differential thermal analysis and thermogravimetric analysis of the BMN powders produced by microwave-assisted hydrothermal processing.

the morphological properties of BMN ceramics, as microwaving increases the particle size enormously if compared with the powders produced by conventional heating. Thermal stability of the BMN phase was studied by DTA−TGA analysis, and the results for the powders produced by microwave-hydrothermal synthesis are shown in Figure 7. Thermal weight loss (TGA curve) was gradual along the temperature range and a higher weight variation was detected in the temperature range 345−385 °C. Besides, the DTA signal, which measures the temperature difference between the sample to be investigated and a reference sample as a function of temperature, presented an endothermic peak at around 370 °C associated with thermal decomposition of residual oxalates from the niobium source ($NH_4H_2[NbO(C_2O_4)_3] \cdot 3H_2O$). DTA is a powerful tool to investigate and control reactions and processes that are thermally activated, showing characteristic temperatures and providing qualitative statements on heat due to chemical reactions. DTA was also used to investigate BMN ceramics produced by conventional hydrothermal synthesis. Similar results were observed, meaning that the presence of residual oxalates is a direct function of the reagent used and not of the processing itself.

The presence of residual oxalates in the hydrothermal powders was investigated by FTIR measurements. Infrared spectroscopy is a valuable tool for elucidating the structures of complex ions in aqueous solutions, as well as for identifying the components, or measuring the concentrations of molecules, in solid samples. In fact, FTIR is very sensitive to the presence of chemical functional groups in a given material and was employed in the present work to detect residual oxalate groups resulting from the hydrothermal processing of BMN ceramics. Fresh powders, as well as samples calcined after complete thermal decomposition of the residual oxalates (600 °C, Figure 7), were subjected to infrared characterization. The results are shown in Figure 8, where the vibrational frequencies of the groups OH, Me−OH, and Me−O can be seen, respectively, in 3450 cm^{-1} (with a strong absorption at 3750 cm^{-1} attributed to singly coordinated OH), 1300−1500 cm^{-1}, and in the broad band below 1000 cm^{-1}. It is important to note that the presence of OH groups (associated to water) in calcined samples is really expected, as a diffuse reflec-

(28) Yoshimura, M.; Suchanek, W. *Solid State Ionics* **1997**, *98*, 197.

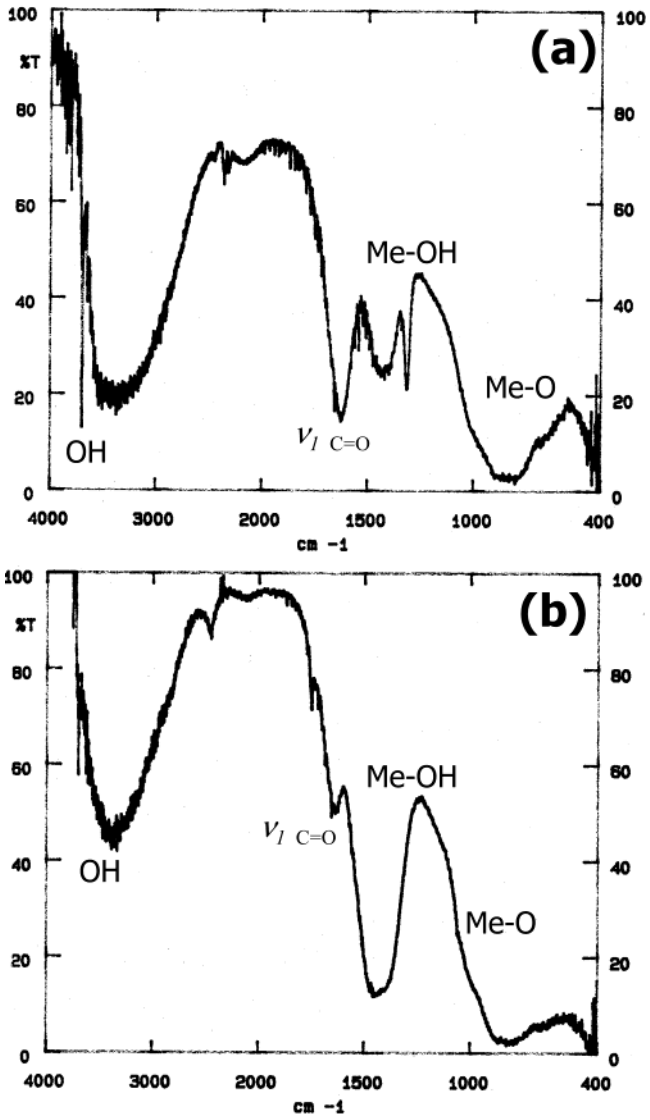

Figure 8. Fourier transform infrared spectroscopy analyses for the BMN ceramics: (a) microwave-hydrothermal powder and (b) calcined sample at 600 °C.

tance apparatus was employed, which is very surface-sensitive. An intense absorption band is observed to occur at 1650−1700 cm^{-1} (Figure 8a), which disappeared after heating at 600 °C (Figure 8b). According to Nakamoto,[29] the oxalate group coordinates to a metal as a unidentate or bidentate ligand, acting as a bridging group between metal atoms. For compounds of the type $[M(C_2O_4)_3]^{-3}$, the spectral signature of the C═O group (ν_1 stretching vibration) appears as an intense band between 1640 and 1670 cm^{-1},[29] as verified in our BMN samples. These observations confirm the results of the thermal analysis reported above, and were also verified by Robertz et al.[30] in their study about the importance of soft solution processing for barium zirconate materials. In fact, there is an amount of oxalate attached to the surface of our BMN powders, but the results indicated that only a residual quantity is present, because the mass loss during heating was very small, and also because the X-ray diffraction did not show any secondary phase contamination or unreacted material.

The hydrothermal technology was next employed to produce lead tungstates, a promising electroceramic for utilization in electromagnetic calorimeters.[21,22] The goal here was to identify hydrothermal conditions to produce crystalline powders with different morphologies and, consequently, different reactivities during sintering. In previous works,[31,32] theoretical simulations were carried out to optimize the experimental procedures for the production of strontium and nickel tungstates. Single-phase and impurity-free powders were obtained under different hydrothermal conditions through dissolution and reprecipitation mechanisms and low temperatures. For $PbWO_4$, computer simulations and hydrothermal experiments were accomplished by using lead nitrate, sodium tungstate hydrate, nitric acid, and sodium hydroxide as raw materials. The hydrothermal syntheses were theoretically modeled in temperatures ranging from 110 to 260 °C, and reagent molal concentrations between 10^{-10} and 10^{0} in the whole pH range. In a general way, the results showed that the most suitable conditions to produce $PbWO_4$ are reagent concentrations higher than 0.03 *m* and pH around 6. Also, it was verified that the conditions for complete precipitation become narrower as the temperature increases, as a result of the increased stability of the solid species PbO. By using computer modeling, it was possible to design and control the production of lead tungstates, avoiding any precipitation of PbO and focusing the morphological control under optimized hydrothermal conditions. The experimental syntheses were accomplished starting from the results obtained by computer simulations at 170, 200, 230, and 260 °C. X-ray diffraction analyses showed that phase-pure lead tungstates (tetragonal phase, ICDD card 19-0708) were obtained for the temperatures tested. The lattice parameters were calculated by using the main reflection planes. It was verified that lower lattice parameters were observed for lower hydrothermal temperatures and times, as expected. For the sample produced at 170 °C for 1 h, the lattice parameters were $a = 5.44$ Å and $c = 11.99$ Å, whereas values closer to the theoretical (ICDD 19-0708) were observed for the samples produced at 260 °C for 4 h ($a = 5.46$ Å and $c = 12.06$ Å). Energy-dispersive spectrometry and X-ray fluorescence analyses showed that impurity-free powders were produced.

Scanning electron microscopy was employed to study the morphological features of the samples. Figure 9 presents the micrographs for the hydrothermal $PbWO_4$ obtained for 1 h (left) and 4 h (right) at temperatures varying from 170 (Figure 9a) to 260 °C (Figure 9d). The influence of the hydrothermal conditions (both temperature and time) on the morphological characteristics of these powders is clear. Lower hydrothermal temperatures and times promoted the formation of a three-dimensional growth structure (dendrite-like), whereas higher temperatures and times tend to modify the particle shape leading to a more rounded powder. The sequence of micrographs in Figure 9 for powders obtained for 4 h (right micrographs) shows the power of the hydrothermal technology to modify the morphologi-

(29) Nakamoto, K. *Infrared and Raman Spectra of Inorganic and Coordination Compounds*; John Wiley and Sons: New York, 1978.
(30) Robertz, B.; Boschini, F.; Cloots, R.; Rulmont, A. *Intl. J. Inorg. Mater.* **2001**, *3*, 1185.
(31) Ciminelli, V. S. T.; Dias, A. *Ferroelectrics* **2000**, *241*, 271.
(32) Dias, A.; Ciminelli, V. S. T. *J. Eur. Ceram. Soc.* **2001**, *21*, 2061.

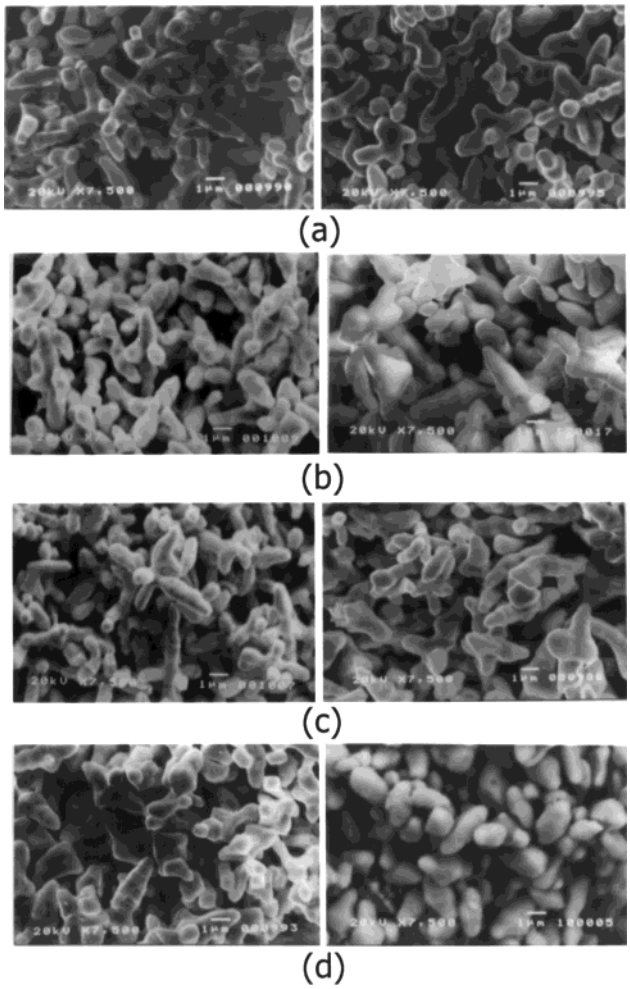

Figure 9. Micrographs for the hydrothermal $PbWO_4$ obtained in conventional reactors at (a) 110 °C; (b) 170 °C; (c) 230 °C; and (d) 260 °C, for 1 h (left) and 4 h (right).

cal features of a given material: by changing the temperature, for example, it was possible to produce shaped materials that, in turn, will present different reactivities during sintering, and, consequently, different microstructures and final properties. It is well-known that the shape of a crystal is determined by the difference in relative growth rates of the individual crystal planes, and the resulting particles are normally bound by facets with the lowest growth rate under a certain supersaturation.[10,28,33] Supersaturation is a function of various experimental parameters such as solution pH, temperature, reagent concentration, and agitation. As supersaturation level increases with hydrothermal temperature, the particles precipitate relatively rapidly from a highly saturated solution due to greater driving force. Consequently, the particles tend to grow into an isotropic shape. For the lead tungstates obtained in the present work, the average particle size did not vary significantly with the hydrothermal conditions, so that only their shape can be considered as different (Figure 9).

Another important morphological parameter that affects the sinterability of a ceramic material is the agglomerate size.[7,32] In this work, this parameter was studied for all $PbWO_4$ samples by using the electrical sensing zone method. This technique determines the number and size of particles suspended in an electrolyte (0.05 wt % of sodium metaphosphate) by causing them to pass through a small orifice on either side of which is immersed an electrode (aperture size of 15 μm and current of 600 μA). The changes in resistance as particles pass through the orifice generate voltage pulses whose amplitudes are proportional to the volumes of the particles (designated ASTM 3365-74T). According to the electrical sensing zone technique, we can obtain the mean agglomerate size by assuming spherical shape particles and an equivalent diameter (D_{50}) is obtained. For the lead tungstates studied in this work, we have obtained similar results for all materials, independent of the residence time in the autoclave (the mean D_{50} value was equal to 2.6 μm and 3.1 μm for ceramics produced for 1 h and 4 h, respectively). Also, a little influence of the hydrothermal temperature on the mean agglomerate size was verified: it tends to increase, and the agglomerate size distribution becomes narrower, as the temperature increases.

Finally, the specific surfaces of the hydrothermal lead tungstates were determined by nitrogen adsorption technique and also inferred by electrical sensing zone method. For these measurements, the true density of the powders was determined by helium pycnometry. It was verified that the materials presented similar density values independently of the hydrothermal conditions employed ($\rho = 8.5 \pm 0.3$ g/cm^3). The adsorption isotherms presented characteristics of mesoporous materials with mean sizes lower than 2 nm, as determined by the pore-size distribution curves. S_{BET} presented a decreasing tendency as the temperature or time increased, as expected for hydrothermal powders.[11,27] The values varied from 0.68 m^2/g for the sample obtained at 170 °C for 1 h, to 0.32 m^2/g for the $PbWO_4$ produced at 260 °C for 4 h. Electrical sensing zone measurements also give us specific surface areas calculated from the agglomerate size distributions assuming materials of spherical shape. For samples obtained at 170 °C for 1 h, the mean value was 0.29 m^2/g, whereas for powders obtained at 260 °C for 4 h the surface areas presented a mean value of 0.26 m^2/g. If you compare these values with those obtained by nitrogen adsorption analyses, it is clear that the proximity between the values observed for higher residence times is intimately related with the fact that rounded shaped powders were hydrothermally obtained only for these conditions. Also, more compact powders or less porous materials were obtained in high temperatures and times.

Conclusions

Hydrothermal technology was employed to synthesize advanced ceramic materials. First, the goal was to show the versatility of this technology to control the structural phases of two ceramic systems. For the perovskite system Na−Nb−H_2O, a mixture of phases was observed at temperatures higher than 110 °C. Cubic $NaNbO_3$ could be produced only at temperatures below 100 °C, whereas orthorhombic and rhombohedral $NaNbO_3$ phases were observed in temperatures higher than 240 °C. For the system Ba−Zr−H_2O, it was verified that there is a clear tendency to produce ideal cubic perovskites ($BaZrO_3$) at higher temperatures. Tetragonal Ba_2ZrO_4

(33) Dirksen, J. A.; Ring, T. A. *Chem. Eng. Sci.* **1991**, *46*, 2389.

and $Ba_3Zr_2O_7$ phases were obtained with the cubic phase at temperatures below 170 °C. Following, the morphological control after the understanding of the phase behavior of a given ceramic system was presented as a second stage in the hydrothermal technology. Barium hafnium oxide was produced for the first time by using conventional hydrothermal reactors at 200 °C, and morphological analyses showed a polyhedral material with open cylindrical mesopores on the pore-network structure. Conventional and microwave-assisted hydrothermal reactors were used to produce BMN powders. Although there are no differences in terms of phase behavior, the powders are morphologically quite different. Nanostructured needle-shaped particles were observed in powders produced in conventional reactors, but microwave-produced ceramics were formed as large needles. Thermal analysis and FTIR detected the presence of residual oxalate groups from the niobium source, which decomposed at 370 °C. $PbWO_4$ ceramics were also produced by conventional hydrothermal processing. Phase-pure and impurity-free powders were obtained with different morphologies. Lower hydrothermal temperatures led to dendrite-like particles, whereas higher temperatures tended to produce rounded shape powders.

Acknowledgment. We acknowledge the financial support from CNPq (Profix 350042/02-0 and 540008/01-0, and Universal 476912/01-6) and Millennium Institute: Water, a mineral approach (CNPq 62.0060/01-8). Thanks also to Dr. Yves Robert Pierre Maniette, from UNESP-Araraquara, for help in carrying out TEM analyses.

CM0210187